Food Research International 43 (2010) 329–341

Contents lists available at ScienceDirect

Food Research International

journal homepage: www.elsevier.com/locate/foodres

Effect of processing history on the functional and structural characteristics of starch–fatty acid extrudates

S.N. Raphaelides *, K. Arsenoudi, S. Exarhopoulos, Z.-M. Xu

Food Process Engineering Laboratory, Department of Food Technology, ATEI of Thessaloniki, P.O. Box 141, Thessaloniki GR-57400, Greece

ARTICLE INFO

Article history:
Received 13 April 2009
Accepted 22 October 2009

Keywords:
Starch–lipid interactions
Extrusion of starch
Extruded starch functionality
Starch extrudate crystallinity

ABSTRACT

Normal maize starch was extruded with and without the addition of fatty acid potassium salts in a twin screw cooker extruder equipped with a slit die rheometer, at 100, 120, 140 or 160 °C barrel temperatures and at screw speeds 20, 91, 161 or 227 rpm. The in line melt viscosity measurements showed that the flow behaviour of the starch system was influenced by the addition of either myristic or palmitic acids used. The examination of functional properties of the extrudates such as bulk density, water solubility index, expansion ratio, degree of gelatinization and water adsorptivity indicated that the addition of fatty acids affected the functionality of starch systems. That is, the extrudate texture became more cohesive and compact whereas the water solubility exhibited by the system was decreased. Structural studies indicated that the crystallinity of starch–fatty acid extrudates was higher than that of the starch systems without fatty acid whereas all extrudates exhibited high glass transition temperatures and their structure was very rigid and brittle.

1. Introduction

Food cooker extruders can be regarded as bioreactors in which thermal and mechanical energies are applied to raw materials, such as native starch. They cause many physical and chemical transformations in starch granules which result in changes of the functional and morphological characteristics of the extrudate products.

The use of a cooker extruder to modify the structure of starch in the presence of lipids has been explored by a number of researchers over the last 30 years. Thus, the formation of amylose–lipid complexes during extrusion cooking, in a twin screw extruder, of starch with added fatty acids, monoglycerides, emulsifiers and various fats was investigated by Mercier, Charbonniere, Grebaut, and de la Gueriviere (1980), Colonna and Mercier (1983), and Meuser, van Lengerich, and Stender, (1985a, 1985b). On the other hand, single screw extruders were also employed to prepare starch–lipid extrudates and to study their physicochemical characteristics (Bhatnagar & Hanna, 1994, 1997; Stäger, 1988; Willett, Jasberg, & Swanson, 1995).

The results reported by the above mentioned researchers are in certain cases conflicting largely due to the different experimental conditions employed by them, such as barrel temperature, screw speed, screw configuration, feed rate, and especially the type of extruder being used, i.e. either with one or two screws. The objective of the present work was to study in a systematic way the effect of fatty acid addition on the functional and structural characteristics of native maize starch extrudates as being influenced by a variety of processing conditions employed.

2. Materials and methods

2.1. Materials

Commercial maize starch was purchased from Nestlè Hellas, Greece. The starch characteristics were: moisture content 12.0%,[1] apparent amylose 21.5 ± 0.6%,[2] total amylose 26.0 ± 0.3%,[2] onset gelatinization temperature 67.5 ± 0.6 °C,[3] peak gelatinization temperature 72.0 ± 0.5 °C.[3]

Myristic acid (purity > 98.5%) was purchased from Fluka, palmitic acid (purity > 95%) was purchased from Sigma Chemical Co. Salts used to prepare solutions of known water activity were: LiCl (>99%), $MgCl_2 \cdot 6H_2O$ (>99%), K_2CO_3 (>99%), $Mg(NO_3)_2$ (>99%) purchased from Fluka, NaCl (>99%) obtained from Merck and KNO_3 (>99%) from Riedel-de Haën. All other reagents used were of analytical grade.

[1] Gravimetrically determined by heating the samples at 130 °C for 1 h.
[2] Determined using the method of Morrison and Laignelet (1983).
[3] Onset and peak gelatinization temperatures measured with a Perkin–Elmer DSC-6 differential scanning calorimeter.

* Corresponding author. Tel.: +30 2310 791371; fax: +30 2310 791360.
E-mail address: rafael@food.teithe.gr (S.N. Raphaelides).

0963-9969/$ - see front matter © 2009 Elsevier Ltd. All rights reserved.
doi:10.1016/j.foodres.2009.10.016

2.2. Extrusion conditions

Extrusion cooking was performed in a pilot scale co-rotating intermeshing twin screw extruder, Clextral model BC45, France. The barrel was 550 mm in length and 110 mm in diameter, with two heating zones heated with induction heaters and cooled with circulating tap water. At the barrel's end, a slit die rheometer was attached through a transition attachment having the shape of a truncated conical neck to provide smooth hydrodynamic transition from the extruder to the die entrance. Both the neck and the slit die rheometer were custom made in a local workshop. The length of the neck was 120 mm and that of the rheometer was 250 mm. The rectangular cross section of the slit die was 20 mm wide and the height was 1.5 mm. Both the neck and the rheometer were equipped with centrally placed type K thermocouples. The rheometer was also equipped with high temperature Gefran, Italy (SP830 M series), pressure transducers, flush mounted along the length of the die with pressure range 0–20 and 0–10 MPa respectively. The rheometer was heated by means of electric cartridge heaters which covered all the available external surface of the rheometer and cooled by means of circulating tap water.

All process variables, i.e. temperatures measured at every zone of the barrel, the neck and the rheometer, pressures from the pressure transducers, rotational speed of the screws, current and power input from the extruder's motor were continuously logged, in real time mode, on a PC through a data acquisition card constructed, and programmed by one of us (Xu) at our electronics workshop. The solid feed was transferred from a hopper, mounted on the extruder, through a controlled speed screw feeder to an opening located in the entrance of the barrel whereas the liquid feed was transported to the opening of the barrel's entrance by means of a metering diaphragm pump from a temperature controlled jacketed vessel equipped with a variable speed stirrer.

2.3. Experimental design

In all experimental runs the extruder was operated in the starve fed mode. The degree of fill, expressed as *g* of feed material/rpm of screw speed (van Lengerich, 1989) was kept constant at 3.0. As for the solid/liquid ratio of the feed material, it was 2:1 in all experimental runs.

Three series of samples were obtained from the respective experimental runs. That is:

- *1st run*: The feed material was a mixture of starch and water (control).
- *2nd run*: The feed material was a mixture of starch and aqueous solution of potassium myristate salt.
- *3rd run*: The feed material was a mixture of starch and aqueous solution of potassium palmitate salt.

The fatty acid concentration corresponded to 1.76% of the starch solids. The feed solution (either with or without fatty acid) was kept, under continuous stirring, throughout the experiments at 60 °C to avoid micelle formation in the feed vessel.

2.4. In line viscosity determination of the extrudate melts

Melt viscosity determination was based on the process parameters recorded on line through out the course of the extrusion processing runs. The rheological equations used were obtained from Han's (1976) analysis.

That is, the shear stress was calculated from the equation

$$\tau = \Delta P * H/2 * L(\mathrm{Pa}) \quad (1)$$

where ΔP is the pressure drop between the pressure sensors; H, the height of the slit (mm); and L is the distance between the pressure sensors (mm).

The wall apparent shear rate was calculated from the equation

$$\dot{\gamma}_{\mathrm{app}} = 3Q/2B * h^2 \ (\mathrm{s}^{-1}) \quad (2)$$

where Q is the volumetric flow rate in the slit (mm^3/s); B, the width of the slit (mm); and h is the ½ of the slit height (mm).

The corrected shear rate was calculated according to the method of Rabinowitsch (Han, 1976) as follows:

$$\dot{\gamma}_{\mathrm{corr}} = (2n + 1/3n) * (3Q/2B * h^2)(\mathrm{s}^{-1}) \quad (3)$$

where n is the flow behaviour index $(\partial \ln \tau)/(\partial \ln \dot{\gamma}_{\mathrm{app}})$, the rest of the symbols are the same as in Eq. (2).

The apparent viscosity was calculated from the power law equation

$$\eta = m * \dot{\gamma}_{corr}^{n-1} \ (\mathrm{Pa} * \mathrm{s}) \quad (4)$$

where m is the consistency index.

All samples after preparation and prior to their examination were stored for 8 days at room temperature so that their moisture content to be equilibrated. Preliminary studies showed that this period of time was quite sufficient for sample stabilization as far as their functional characteristics are concerned.

2.5. Specific mechanical energy (SME)

The extruder was driven by a DC motor powered from 3-phase mains through controlled rectifier of thyristor for speed regulation. The SME provided by the motor of the extruder during the extrusion cooking process was calculated using the following equation:

$$\mathrm{SME} = \mathrm{ME} - \mathrm{TE} = [(V * I) - (I^2 * R)]/m \ (\mathrm{Wh} * \mathrm{kg}^{-1}) \quad (5)$$

where ME is the mechanical energy provided by the motor to the extruder; TE, the thermal loss due to electrical resistance in the motor (Joule effect); V, the voltage applied to the armature of the motor (Volts); I, the current (Amperes); and m is the feed rate supplied to the extruder (kg/h).

Since $(V - IR)$ is proportional to the screw speed, it can be measured from the speed setting signal. The current signal was taken from the meter. Both signals were at mains potential, therefore were fed to the computer connected to the extruder, through opto-coupler for insulation and *V–F*, *F–V* converter signal accuracy.

2.6. Moisture content

It was gravimetrically determined by heating the samples at 130 °C for 90 min.

2.7. Bulk density

It was determined using a volume displacement technique as follows: in a preweighed graduated cylinder, capacity 250 mL, 140 mL of *n*-hexane were added and the cylinder was reweighed. An approximately 12 cm in length of weighed extrudate sample was fully submerged inside the cylinder and by means of a positive displacement mechanical pipette the displaced volume of the *n*-hexane was carefully transferred to a dry preweighed beaker and the beaker was again weighed. Since the density of *n*-hexane is known to be 655 $\mathrm{kg/m}^3$, the volume of the displaced *n*-hexane can be easily and accurately calculated. The volume of the displaced *n*-hexane is equal to the volume of the sample, thus the bulk density of the sample can be calculated by dividing the mass of the sample by its volume. The measurements were replicated three times.

2.8. Expansion ratio

The determination of the cross sectional area of the samples was quite difficult due to irregularities most of them exhibited on their surface. Hence, it was decided to use the following technique: the length of the samples was accurately measured using a digital vernier caliper. From bulk density determination the volume of the sample was known. Thus, dividing the volume by the length, the average cross sectional area of the sample was obtained. This ratio was termed expansion ratio.

2.9. Water solubility index (WSI)

WSI, defined as the water soluble fraction of the extrudate expressed as percentage of dry sample and being a measure of the dispersibility of the material was measured by the method of Anderson, Conway, Pfeifer, and Griffin (1969).

2.10. Adsorption isotherms

Extrudate samples were dried in a vacuum oven at 50 °C for at least 24 h, till constant weight. Quantities (~0.5 g) of the dried samples, contained in preweighed polypropylene dishes, were weighed in an analytical balance and placed over saturated (at 40 °C) salt solutions of known relative humidity values in hermetically sealed glass containers (capacity 800 mL). Then, the containers were stored in a thermostatically controlled chamber at 30 °C. The dishes were weighed, at regular time intervals, till constant weight. It was found that equilibrium was achieved after a week. The adsorption experiments were replicated three times. The adsorption isotherms were drawn using as coordinates the parameters, percentage relative humidity and water content, i.e. the weight difference of the sample at the beginning of the storage period at a certain relative humidity environment and after the equilibrium in this environment was achieved, over the initial weight of the dried sample.

2.11. Degree of gelatinization

The degree of gelatinization of the extrudates was defined as the weight ratio of gelatinized starch to total weight of sample. The determination was based on formation of blue iodine complex by amylose released during starch gelatinization (Birch & Priestly, 1973). According to this method, described by Cai and Diosady (1993), a sample (0.04 g) was dispersed in 50 mL 0.06 M KOH solution and then gently agitated for 15 min. The slurry was centrifuged and 1 mL aliquots of supernatant was removed, mixed with 9 mL 0.00667 M HCl. Then 0.1 mL iodine reagent (1 g iodine and 4 g potassium iodide/100 mL water) was added, and after mixing the absorbance a_1 was read at 600 nm in the spectrophotometer against a reagent blank. The estimation was repeated using 50 mL 0.4 M KOH solution, and 9 mL 0.0445 M HCl to obtain absorbance a_2. As reference material (100% gelatinized), pregelatinized maize starch, prepared by us using a double drum dryer and checked by X-ray diffraction, was employed. The determination was replicated three times.

2.12. Limiting viscosity number (intrinsic viscosity)

Finely cut (thickness 25 μm), in a microtome, pieces of extrudate samples were dissolved in aqueous solution of 1 N KOH, at 60 °C under periodic swirl mixing. The solutions were diluted with distilled water to 0.1 N and then they were filtered through Gooch fritted glass filter No. 2 to remove minute quantities of undissolved particulate material. The specific viscosity (η_{sp}) of the solutions was measured using an Ubbelohde suspended level type viscometer which was kept in a water bath at 20 ± 0.1 °C. The flow time of the solvent (0.1 N KOH) was 130 s. The initial starch concentration of the filtered solutions was around 4 mg/mL, accurately determined using an enzymic method (Karkalas, 1985). The intrinsic viscosity was determined from the gradient by using linear regression on the viscosity number (η_{sp}/c)–concentration (c) data, according to the method described by Greenwood (1964).

2.13. Modulus of elasticity and rheological glass transition temperature

Extrudate samples were cut into strips of dimensions $36 * 10 * 3$ mm and were measured in a DMA rheometer Bohlin CVOR 150, operated in the oscillatory mode under constant frequency 0.1 Hz, constant stress 150 Pa and programmed heating rate of 5 °C/min. The strain in all samples examined ranged from 10×10^{-7} to 10×10^{-5} which was well within the linear viscoelastic region. The parameters measured were the storage modulus G' and tan δ in relation to the temperature of heating.

2.14. X-ray diffraction

Extrudate samples were immersed in liquid nitrogen and immediately were pulverized by means of a pestle and a mortar. The powder obtained was passed through a sieve with an aperture of 800 μm. X-ray powder diffraction measurements were carried out using a PANalytical X'Pert Pro diffractometer with a Cu Ka_1 radiation (λ = 1.5405980 Å). The diffractometer was operated in reflection mode at 45 kV and 40 mA. A divergence slit of 1°, an antiscatter slit of 2° and a receiving slit of 0.4 mm were used. Measurements were taken between 6° and 35° (2θ) with a step size of 0.04° and a scan speed of 0.008 deg/s.

For the determination of the relative crystallinity the data were normalized from 9° to 30° (2θ) and the background was determined using the X'Pert HighScore PANalytical software. The crystallinity index (X_c) was calculated according to the following equation (Stribeck, 2007):

$$X_c = \frac{I_{cr}}{I_{am} + I_{cr}} \tag{6}$$

where I_{cr} is the integrated area between the crystalline reflections and the amorphous halo and I_{am} is the integrated area between the amorphous halo and the baseline.

Crystallite size was determined according to Scherrer's formula (Brundle, Evans, & Wilson, 1992):

$$L \approx \frac{\lambda}{FWHM \times \cos\theta} \tag{7}$$

where L is the crystallite size in Å; λ, the wavelength and $FWHM$ is the Full Width at Half-Maximum.

2.15. Scanning electron microscopy

Extrudate samples were mounted on aluminum stubs with sticky double-side carbon tape. No special treatment applied to the specimens and no coating was needed. Examination was performed by a Carl Zeiss EVO 50 VP scanning electron microscope (Carl Zeiss SMT, Ltd., UK) at 5 kV accelerating voltage, under variable pressure mode, suitable for non-conductive specimens, at pressure of 30 Pa. A Variable Pressure Secondary Electron (VPSE) detector was used.

3. Results and discussion

The experimental scheme applied in all three runs is shown in Table 1.

Table 1
Throughput rates, heating temperatures[a] and screw speeds employed in all extrusion experimental runs.

Sample	Throughput rate (solid + liquid) (kg/h)	Extrusion processing temperature (°C)	Screw speed (rpm)
1	3.60	100	20
2	16.38	100	91
3	29.01	100	161
4	40.81	100	227
5	3.60	120	20
6	16.38	120	91
7	29.01	120	161
8	40.81	120	227
9	3.60	140	20
10	16.38	140	91
11	29.01	140	161
12	40.81	140	227
13	16.38	160	91
14	29.01	160	161
15	40.81	160	227

[a] In all heated sections of the extruder system and for each sample, the selected temperatures were the same.

The quantity of fatty acids used was calculated to be 5% in excess to that needed to fully saturate the available amylose helices (Karkalas & Raphaelides, 1986), provided that all molecules of apparent amylose would be in position to interact freely with the fatty acid molecules. The fatty acids were added to starch as soap aqueous solution in order their molecules to be in their most active form, i.e. as monomers. These precautions were taken since the available water in the starch system was limited and it was imperative to secure the best possible dispersibility of the fatty acid anions so to achieve the maximum degree of interaction between the starch molecules and the fatty acid anions.

3.1. Flow behaviour of starch–fatty acid extrudate melts

Fig. 1 shows the flow curves obtained for the three systems examined, i.e. starch–water (control), starch–myristate soap solution and starch–palmitate soap solution at different slit die temperatures (100, 120, 140, 160 °C). It can be seen that at 100 °C (Fig. 1a) and at fairly low shear rates the viscosities of the two starch–fatty acid systems are higher than that of the control whereas at very high shear rates the viscosity of the palmitic acid containing sample became lower than that of the control. This could be attributed to the fatty acid interaction with amylose and the formation of helical complexes. It is known (Banks & Greenwood, 1971; Carlson, Larsson, Dinh-Nguyen, & Krog, 1979; Godet, Tran, Delage, & Buleon, 1993; Snape, Morrison, Maroto-Valer, Karkalas, & Pethrick, 1998), that the helical cavity is hydrophobic whereas at the outer surface of the helix, active amylosic hydroxyl and fatty acid carboxyl groups are exposed enabling adjacent molecules to interact, possibly through hydrogen bonding, with each other and to form supermolecular structures, i.e. a kind of quaternary structure. Thus, the hydrodynamic volume of the molecular systems increases at relatively low shear rates, whereas at higher shear rates this supermolecular structure tends to be dissociated and the viscosity of the starch–fatty acid systems approaches that of the control. Similar phenomena were observed for starch–fatty acid systems in excess water (~85%) heated at temperatures close to 100 °C (Raphaelides & Georgiadis, 2006). It is worth noting that the viscosity of the control at 100 °C is lower than that at 120 °C, whereas it should have been the opposite (Fig. 1b). This paradox could be attributed to the incomplete gelatinization of starch molecules occurred at 100 °C, due to limited amount of water present and the very short heating time. The data

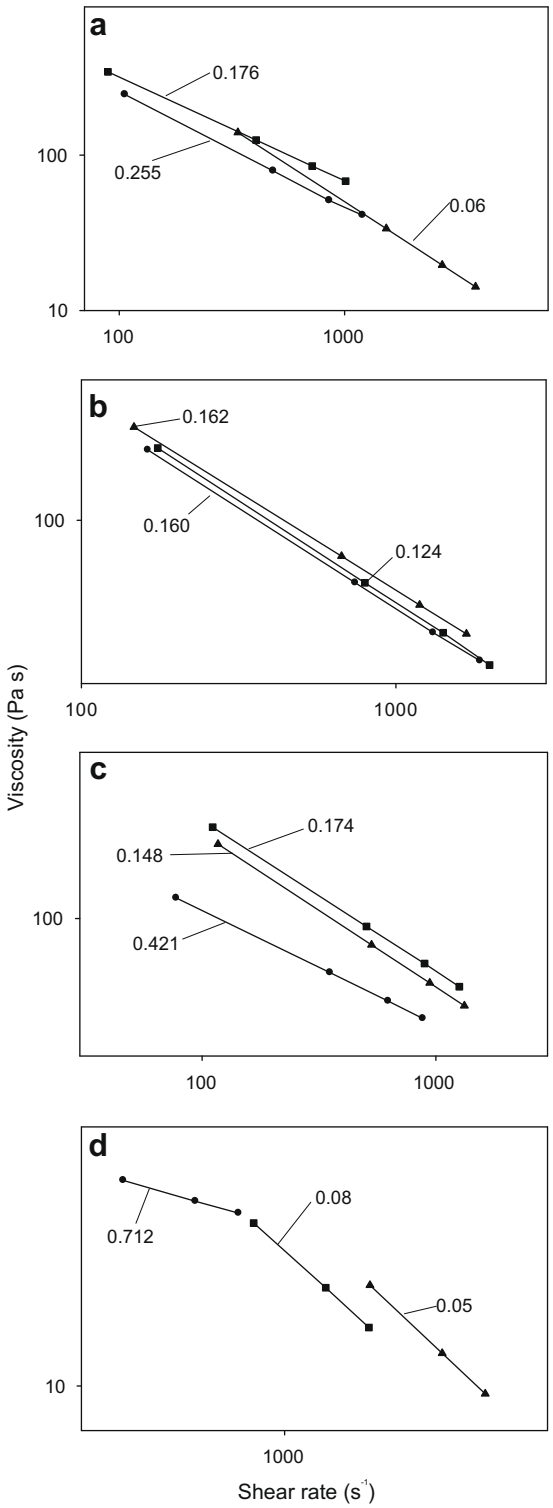

Fig. 1. Effect of heating temperature on the flow behavior of starch–fatty acid extrudate melts. ●, Control sample (no fatty acid added); ■, sample with added myristic acid; ▲, sample with added palmitic acid. (a–d) Denote heating temperatures of 100, 120, 140 and 160 °C respectively. Numbers attached to the flow curves denote the flow behavior index of the individual curve.

obtained from the determination of the degree of gelatinization (Table 2) confirmed this assumption. Similar behaviour was observed in the case of starch–palmitate extrudates where palmitate ions virtually suppress gelatinization. On the other hand, it can be seen that myristic acid seems to promote starch gelatinization.

Table 2
Effect of screw speed and barrel temperature on the functional properties of starch–fatty acid extrudates.

Sample	Screw speed (rpm)	Barrel temperature (°C)	Degree of gelatinization (%)	Moisture content (%)	Bulk density (kg/m^3)	Expansion ratio	Water solubility index (%)
Control	20	100	24.7 ± 2.5	17.8 ± 0.5	1424 ± 5	1.36 ± 0.02	3.0 ± 0.2
Starch + myristate			78.2 ± 2.0	12.0 ± 0.2	1427 ± 2	1.18 ± 0.05	1.9 ± 0.5
Starch + palmitate			7.5 ± 2.5	15.1 ± 0.5	1414 ± 4	1.26 ± 0.07	1.3 ± 0.1
Control		120	45.9 ± 3.5	14.2 ± 0.2	1434 ± 2	1.73 ± 0.05	4.3 ± 0.5
Starch + myristate			101.0 ± 2.5	11.7 ± 0.5	1395 ± 5	1.22 ± 0.01	2.0 ± 0.2
Starch + palmitate			8.2 ± 1.5	15.7 ± 0.5	1414 ± 6	1.27 ± 0.02	2.2 ± 0.3
Control		140	52.3 ± 1.5	15.1 ± 0.5	1275 ± 15	2.29 ± 0.01	13.1 ± 1.5
Starch + myristate			95.0 ± 2.5	12.9 ± 0.1	1399 ± 5	1.52 ± 0.05	2.8 ± 0.5
Starch + palmitate			10.2 ± 1.5	13.0 ± 0.2	1447 ± 8	1.35 ± 0.02	3.0 ± 0.5
Control	91	100	24.3 ± 1.2	14.9 ± 0.2	1396 ± 5	1.51 ± 0.07	2.9 ± 0.8
Starch + myristate			96.7 ± 1.8	14.0 ± 0.5	1458 ± 2	1.29 ± 0.05	1.9 ± 0.3
Starch + palmitate			25.7 ± 0.5	14.3 ± 0.4	1244 ± 4	1.38 ± 0.02	2.2 ± 0.3
Control		120	31.6 ± 2.0	21.6 ± 1.0	1296 ± 3	2.60 ± 0.02	2.0 ± 0.5
Starch + myristate			91.7 ± 3.5	12.7 ± 0.3	1193 ± 4	1.97 ± 0.02	2.6 ± 0.2
Starch + palmitate			10.0 ± 2.5	13.6 ± 0.4	1234 ± 7	1.75 ± 0.01	2.5 ± 0.2
Control		140	47.2 ± 3.0	22.6 ± 0.4	861 ± 2.0	3.49 ± 0.02	0.8 ± 0.2
Starch + myristate			105.0 ± 0.5	13.9 ± 1.0	1284 ± 5.0	2.40 ± 0.02	2.5 ± 0.4
Starch + palmitate			10.4 ± 2.0	14.5 ± 0.8	1320 ± 5.0	2.05 ± 0.05	1.8 ± 0.4
Control		160	60.0 ± 2.0	13.0 ± 0.5	809 ± 5.0	2.12 ± 0.01	16.5 ± 2.0
Starch + myristate			107.0 ± 1.0	9.8 ± 0.8	682 ± 3.0	5.10 ± 0.03	3.4 ± 0.5
Starch + palmitate			24.7 ± 2.0	12.8 ± 0.7	710 ± 6.0	4.29 ± 0.07	2.3 ± 0.4
Control	161	100	26.3 ± 3.0	22.1 ± 1.0	1015 ± 5	2.53 ± 0.03	2.3 ± 0.8
Starch + myristate			81.0 ± 5.0	14.3 ± 0.6	900 ± 8	2.39 ± 0.01	1.3 ± 0.8
Starch + palmitate			10.8 ± 2.0	13.1 ± 0.2	981 ± 3	1.75 ± 0.02	1.9 ± 1.0
Control		120	38.8 ± 1.8	16.7 ± 1.5	708 ± 3	5.85 ± 0.1	18.9 ± 0.3
Starch + myristate			94.0 ± 3.0	15.8 ± 1.0	837 ± 2	2.56 ± 0.07	1.6 ± 0.1
Starch + palmitate			6.3 ± 2.2	14.2 ± 0.8	820 ± 6	2.43 ± 0.03	2.0 ± 0.2
Control		140	43.4 ± 3.5	16.7 ± 1.0	664 ± 4	3.61 ± 0.08	10.2 ± 1.0
Starch + myristate			90.1 ± 3.0	12.4 ± 0.1	780 ± 3	3.50 ± 0.03	2.5 ± 0.05
Starch + palmitate			5.2 ± 1.7	13.6 ± 0.2	875 ± 5	2.69 ± 0.07	0.9 ± 0.02
Control		160	58.3 ± 2.5	15.4 ± 0.4	648 ± 7	2.78 ± 0.04	7.0 ± 1.00
Starch + myristate			105.0 ± 2.0	9.9 ± 0.3	652 ± 5	4.39 ± 0.05	1.6 ± 0.03
Starch + palmitate			8.0 ± 1.0	12.9 ± 0.3	659 ± 2	3.21 ± 0.03	1.1 ± 0.01
Control	227	100	22.5 ± 2.4	24.0 ± 1.4	1007±.4	2.37 ± 0.41	0.4 ± 0.04
Starch + myristate			67.6 ± 5.5	14.3 ± 0.6	920 ± 2	2.18 ± 0.02	1.2 ± 0.02
Starch + palmitate			5.9 ± 1.2	13.8 ± 1.1	917 ± 6	1.98 ± 0.03	1.5 ± 0.14
Control		120	38.3 ± 2.0	11.9 ± 0.4	806 ± 4	4.01 ± 0.04	5.1 ± 0.09
Starch + myristate			81.6 ± 2.4	13.2 ± 0.7	711 ± 7	3.01 ± 0.01	1.5 ± 0.11
Starch + palmitate			3.2 ± 0.6	14.6 ± 0.3	765 ± 5	2.34 ± 0.08	1.8 ± 0.21
Control		140	39.6 ± 1.4	15.4 ± 0.5	686 ± 8	2.66 ± 0.24	9.6 ± 1.4
Starch + myristate			52.0 ± 3.0	12.4 ± 0.8	689 ± 3	2.86 ± 0.11	1.0 ± 0.5
Starch + palmitate			4.3 ± 0.4	13.5 ± 0.1	667 ± 6	2,82 ± 0.04	1.3 ± 0.1
Control		160	34.0 ± 0.7	18.7 ± 0.4	665 ± 2	2.79 ± 0.14	4.6 ± 0.4
Starch + myristate			82.7 ± 1.6	9.6 ± 0.7	649 ± 4	3.77 ± 0.08	1.6 ± 0.2
Starch + palmitate			4.6 ± 0.2	12.7 ± 0.9	663 ± 7	2.98 ± 0.19	0.8 ± 0.3

Similar results were reported (Raphaelides & Georgiadis, 2006) in the case of starch–fatty acid systems heated in excess water (⩾85%). To strengthen the postulation that palmitic acid suppresses starch gelatinization, extruded starch–palmitic acid samples were placed in hermetically sealed Pyrex glass tubes in which excess water was added and the tubes were heat treated at 120 °C for 30 min. Then, the degree of gelatinization was determined as previously described. The results (not shown) indicated that the degree of gelatinization was dramatically increased to 100%, possibly due to the dissociation of starch–palmitate complexes and the removal of the acid molecules from the amylose helical cavity; thus the starch molecules were able to interact freely with iodine. Alternatively, it is possible that due to prolonged heating (30 min) in excess water the starch gelatinization process was successfully concluded. However, it should be noted that as far as the control samples are concerned the method employed, for the determination of the degree of gelatinization, gives relatively satisfactory results while for the samples contained fatty acids the results obtained should be treated with caution since it cannot be secured the iodine ions are in position to quantitatively displace all the fatty acid molecules from the cavity of amylose helices. Thus, the degree of gelatinization measurements could only portray a qualitatively different behaviour between the samples examined.

At higher extrusion temperatures, i.e. 120–160 °C it can be seen (Fig. 1c and d) that again the viscosity of the starch–fatty acid extrudates was higher than that of the control, especially at fairly low shear rates. It has to be noted that the pseudoplasticity of starch–fatty acid extrudates was much higher than that of the control especially at the higher extrusion temperatures employed. This should be attributed not only to the dissociation of the formed super molecular structure, which was previously mentioned, but also due to the orderly arrangement of the elongated amylose helices at high shear rates causing the significant reduction in viscosity.

3.2. Specific mechanical energy (SME)

The amount of SME input during the extrusion process is considered as an indication of the severity of the structural modifications the feed material undergoes during extrusion. It has been reported (Della Valle, Kozlowski, Colonna, & Tayeb, 1989; van Lengerich, 1989) that starch fragmentation occurs as the result of mechanical energy input and the medium molecular weight of extruded starch decreases as the SME value increases.

Fig. 2 shows the SME input at the specified barrel temperatures during the extrusion of maize starch–fatty acid systems in relation to screw speed. It can be seen that as far as the control (starch and water mixture) is concerned, SME input was both barrel temperature and screw speed dependent. That is, the higher the extrusion temperature, the higher was the SME input and the higher the screw speed employed the higher the SME attained. However, the addition of fatty acids caused, in all cases, less dramatic effects in SME input than those observed in the control samples. That is, the SME slightly increased as the screw speed increased at 100 °C barrel temperature whereas it remained fairly constant at higher temperatures regardless of the screw speed employed. Thus, if we consider that the low values of SME are due to the presence of fatty acids in the starch extrudates then it means that starch macromolecules undergo less severe degradation during extrusion in the presence of lipids in comparison to that occurred in the absence of lipids. Colonna and Mercier (1983) reported that the addition of lipids such as lecithin, copra oil, oleic acid and monoglycerides in manioc starch, caused limited degradation to starch macromolecules during extrusion. To evaluate starch degradation they employed the techniques of intrinsic viscosity and gel permeation chromatography. They suggested that the lipids acted as lubricants which minimized the shearing effect of the extrusion process on the macromolecular structure of starch. Bearing in mind these assumptions our view is that the low SME values observed for the starch–fatty acid extrudates are rather not due to the lubrication effect of the lipids but are related to conformational changes the starch macromolecules underwent due to starch–fatty acid interactions. It is known (Karkalas & Raphaelides, 1986; Raphaelides, 1992) that the formation of amylose–fatty acid complexes in solution, changes the conformation of amylose from random coil to helix thus reducing the hydrodynamic volume of starch macromolecules. Thus, especially at high barrel temperatures and at high screw speeds where the pseudoplasticity of the molten starch systems became more pronounced (Fig. 1) the flow of the melt through the slit die became a lot easier resulting in maintaining SME input at fairly low levels.

3.3. Intrinsic viscosity

Intrinsic viscosity ($[\eta]$) as a measure of starch degradation (depolymerization) during extrusion, has been used by a number of workers (Colonna, Doublier, Melcion, de Monredon, & Mercier, 1984; Colonna & Mercier, 1983; Davidson, Paton, Diosady, & Larocque, 1984; Launay & Konê, 1984). Moreover, it has been reported (Della Valle et al., 1989; Parker, Ollett, & Smith, 1990) that SME is inversely related to intrinsic viscosity. Fig. 3 shows the $[\eta]$ values exhibited by starch–fatty acid extrudates as a function of barrel temperature and screw speed. The $[\eta]$ of native maize starch determined under the same experimental conditions employed for the extrudate samples, was found to be 144.50 mL/g. It can be seen, that all extrudate samples regardless of whether they contained fatty acid or not showed lower $[\eta]$ values than that of the native starch. This is an indication that all extrudates have undergone a certain degree of starch modification, possibly degradation. At the first two specified barrel temperatures, i.e. 100 and 120 °C the $[\eta]$ values of the fatty acid contained samples are lower than the respective ones of the control samples. This is puzzling since if we take into account the respective SME values (Fig. 2) and the findings of Della Valle et al. (1989) that the intrinsic viscosity is inversely proportional to SME, then the fatty acid containing samples

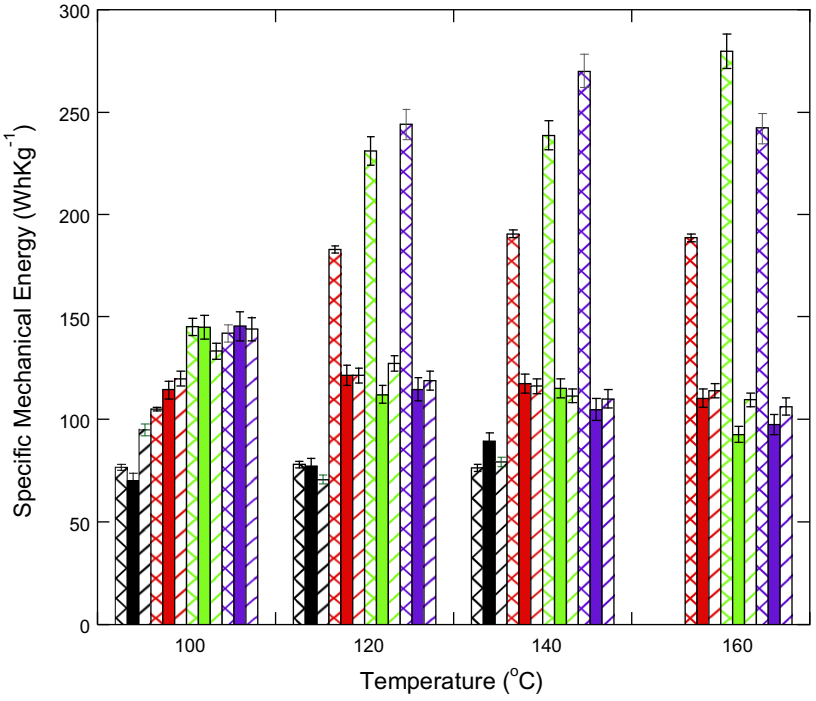

Fig. 2. Effect of screw speed and barrel temperature on the specific mechanical energy of starch–fatty acid extrudates. Crossed line columns: control samples (no fatty acid added); filled columns: samples with added myristic acid; inclined line columns: sample with added palmitic acid. Column colours denote screw speeds: black, 20 rpm; red, 91 rpm; green, 161 rpm; blue, 227 rpm. (For interpretation of the references to colour in this figure legend, the reader is referred to the web version of this article.)

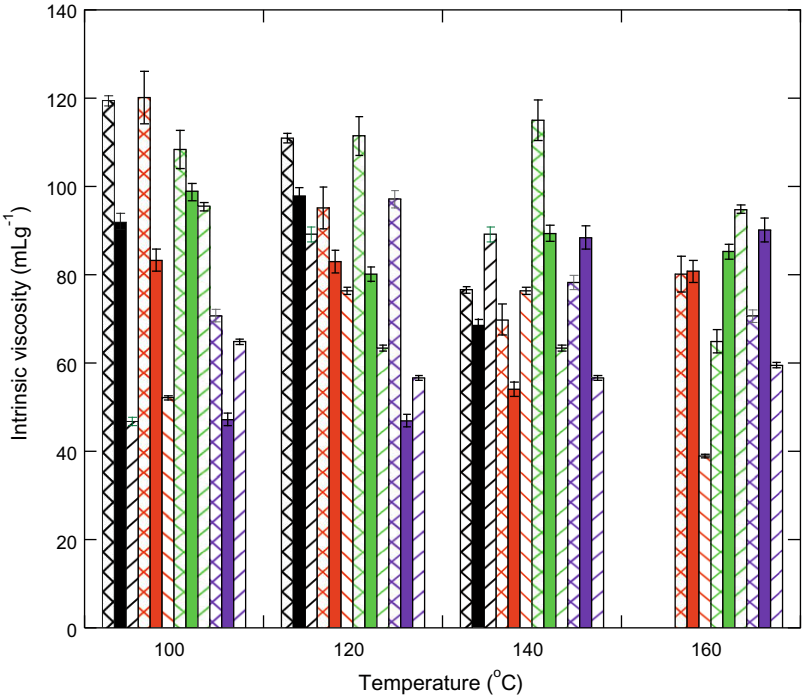

Fig. 3. Effect of screw speed and barrel temperature on the intrinsic viscosity of starch–fatty acid extrudates. Symbols are the same as in Fig. 2.

should have exhibited higher [η] values as long as they showed lower SME values than the respective control samples. However, it has been previously demonstrated (Karkalas & Raphaelides, 1986) that the intrinsic viscosity of amylose molecules was dramatically reduced in the presence of added fatty acids, due to amylose–fatty acid interactions which caused changes in amylose's conformation from random coil to helix resulting in the significant reduction to its hydrodynamic volume. Thus, the intrinsic viscosity should be considered with caution when it is used as a tool for assessing starch degradation at least in cases where in the starch system under examination there is an amylose complexing agent.

At the present work, in the case of control samples the naturally present fatty acid content of the native starch is quite low to cause any appreciable changes in the hydrodynamic properties of starch molecules thus intrinsic viscosity can be considered with confidence as a proof that the starch molecules underwent degradation (depolymerisation) during extrusion. On the other hand, this is not valid in the case of fatty acid contained starch samples. What someone can argue in this case is that the starch–fatty acid extrudates do show a kind of structural modification which nevertheless is not necessarily due to degradation.

3.4. Functional properties of starch–fatty acid extrudates

Table 2 shows the moisture contents of starch–fatty acid extrudates at various screw speeds. It can be seen that the moisture content of control samples, in general, is higher than that of the starch–fatty acid samples. This is possibly due to the formation of the crystalline type II polymorph V-structure of the amylose–fatty acid complexes which is known (Biliaderis & Seneviratne, 1990) to be very compact, thus fewer water molecules remained trapped among the amylose helices. The lower moisture content of the samples extruded at higher temperatures could be attributed to water evaporation occurred at the exit of the die due to the high temperature difference between the extruder's die interior and the atmospheric environment. It has to be noted that samples contained myristic acid had lower moisture content than the rest possibly due to more efficient complexation of amylose–myristate ions (Meuser et al., 1985a) hence the formation of a more compact structure in comparison to the other samples.

The effect of temperature on the bulk density of starch–fatty acid extrudates is also shown in Table 2. It can be seen that the most pronounced changes were exhibited by the control samples whereas the fatty acid containing samples exhibited similar behaviour throughout the temperature range employed. The bulk density changes, it appears to be residence time as well as extrusion temperature dependent. That is, samples extruded at high temperatures and at high screw speeds showed lower bulk density due to their swelling at the exit of the die, thus creating a rather open structure. At fairly low screw speeds, i.e. 20 and 91 rpm the fatty acid containing samples exhibited exceptional stability in their bulk density which remained quite high at least up to 140 °C. This could be attributed to the increase of elasticity of the starch system due to amylose–fatty acid interactions which helped the structure of the system to withstand the high shear forces developed during extrusion without being collapsed. It has been reported (Raphaelides, 1992) that the addition of fatty acids to starch solutions, in quantities sufficient to saturate the available amylose helices, increased the elasticity exhibited by starch systems in solution, expressed in the form of normal force measurements during steady shear experiments.

The changes in expansion ratio of starch–fatty acid extrudates as a function of extrusion temperature (Table 2) revealed that the fatty acid containing samples showed a concomitant gradual increase of expansion ratio with the increase of extrusion temperature. On the other hand, the control samples showed the same tendency at low screw speeds, i.e. relatively long residence time, where as the speed increased the expansion ratio increased in parallel with the extrusion temperature up to a certain extrusion temperature and then it was reduced possibly due to structure collapse at high shear rates and elevated temperatures. This difference in behaviour between the control and the fatty acid containing extrudates could be, again, attributed to the development of a more cohesive structure in the starch–fatty acid systems which being

more elastic withstands better the high shearing forces acting upon them during extrusion as previously mentioned.

As for the changes in water solubility index (WSI) in relation to extrusion temperatures employed at various screw speeds, it can be seen (Table 2) that all fatty acid containing samples exhibited very low WSI values regardless of the extrusion temperature as well as of the screw speed. Similar results were reported by other researchers as well (Bhatnagar & Hanna, 1994; Colonna & Mercier, 1983; Mercier et al., 1980; Meuser et al., 1985b; Stäger, 1988). This indicates the very compact and cohesive structure formed due to starch–fatty acid interactions which makes it very difficult the water molecules to penetrate the starch system matrix and to solubilize it. Moreover, it shows that due to the elastic behaviour exhibited by the starch–fatty acid systems during extrusion they were able to withstand the applied high shearing forces thus avoiding molecular degradation which otherwise would have resulted in increased water solubilization of the extrudates. On the other hand, in the case of the control samples, WSI was low at rather low extrusion temperatures and low screw speeds, whereas at high temperatures the WSI increased. In contrast, at high screw speeds, at rather low extrusion temperatures the WSI increased whereas at high temperatures decreased. This behaviour might be due to the higher hydrodynamic volume acquired by the starch–water system during extrusion in comparison to that of the starch–fatty acid–water system, which favored the disruption of the starch molecules thus increasing the mass fraction which was prone to water solubilization.

Adsorption isotherm experiments indicated (data not shown) that the behaviour of all extrudate samples regardless of whether they contained lipids or not, was the same. Limited moisture adsorption was observed for all extrudate samples even at high relative humidity values. Attempts were made to find out whether sorption isotherm models such as GAB, BET or others could be used to describe the isotherms. Nevertheless, it was found that non model satisfactorily fits for a fairly wide range of relative humidities. Especially, one of the GAB parameters was found to have negative values for all isotherms examined and this was rejected because of physical impossibility. This deviation from the model

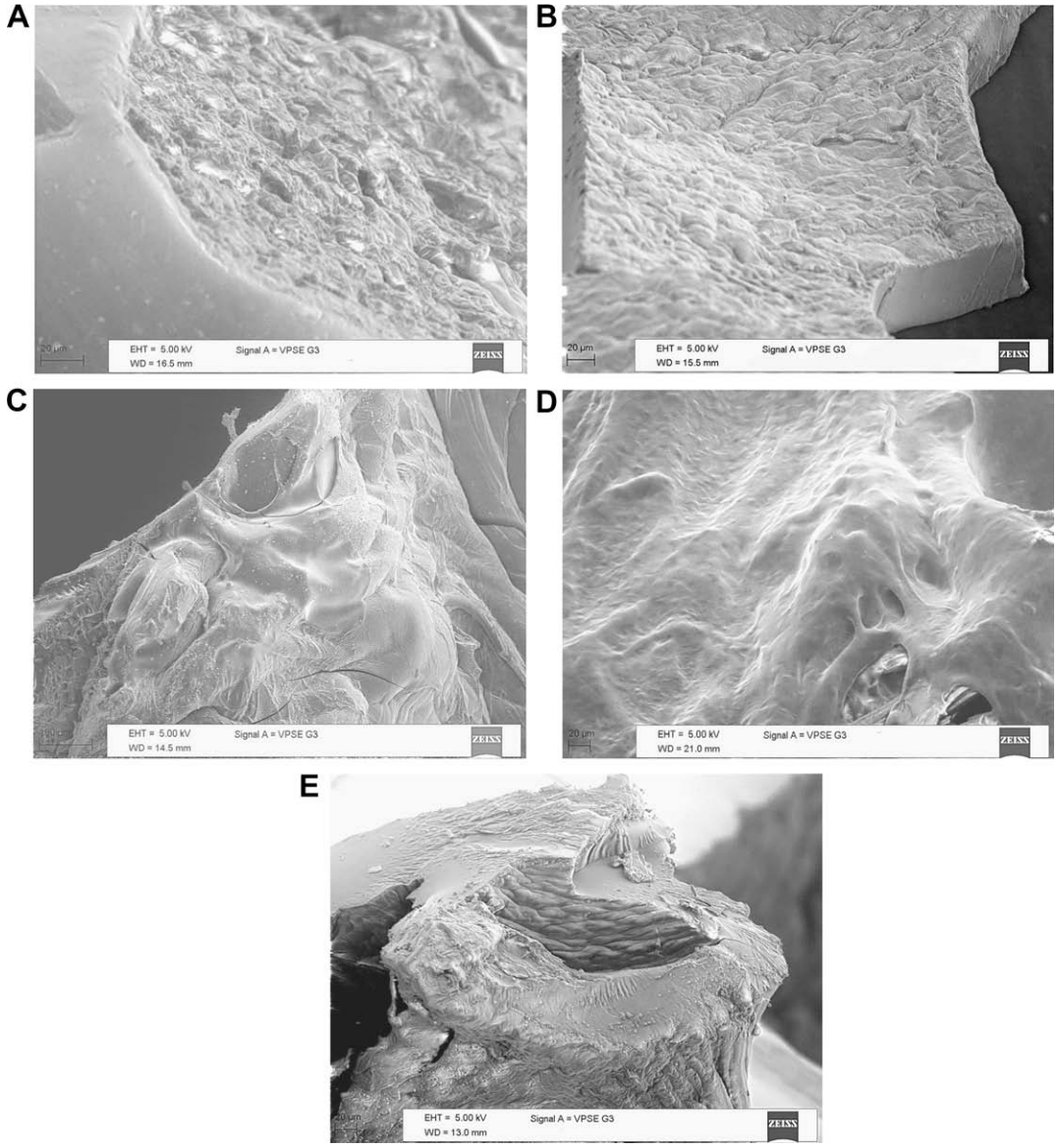

Fig. 4. SEM micrographs of maize starch extrudates with added myristic acid and without (control). (A) Control extruded at 100 °C and at 20 rpm screw speed; (B) starch–myristic acid extruded at 100 °C and at 227 rpm; (C) control extruded at 160 °C and at 91 rpm; (D) control extruded at 160 °C and at 227 rpm; (E) starch–myristic acid extruded at 160 °C and at 227 rpm.

should be attributed to the crystallinity exhibited by the extrudates with or without the addition of lipids. Bizot (1983) emphasized that for starch the GAB model does not fit when it becomes more crystalline at water activities from 0.6 to 0.7.

3.5. Scanning electron microscopy

Extrusion processing is known to cause substantial changes in the physical characteristics of starch granules. That is, extruded starch has lost its granular structure and the structural form it acquires depends on the operating conditions employed during extrusion. Fig. 4 shows the typical photomicrographs of control samples and starch–myristate extrudates. It can be seen that in all samples the granular form of starch is completely absent regardless of the operating conditions employed. At 100 °C both control and starch–myristate extrudates show cells which were not ruptured. However, at 160 °C the structure of the starch–myristate sample became denser than that of the control which acquired a much more open structure than that it had at lower barrel temperature. Similar results have been reported by Bhatnagar and Hanna (1997).

3.6. X-ray diffraction

It has been known (Mercier, 1980) that extrusion cooking modifies the crystalline pattern exhibited by maize starch when the starch is extruded at temperatures over 70 °C. The A-type pattern characteristic of native cereal starches gradually transforms, during extrusion cooking, to the so called V-pattern which is characteristic of the amylose–lipid complex crystalline structure. Besides, when a lipid is added to starch during extrusion cooking, the extrudate gives the V-type pattern whose characteristic peak, at approximately 19.5° (2θ), becomes very pronounced. Fig. 5 shows a typical example of how the X-ray pattern of native maize starch which has been extruded at 140 °C and at screw speed 227 rpm, was transformed to a weakly defined V-pattern due to amylose complexation with the naturally occurred lipids and how this pattern became more pronounced when myristic or palmitic acids were added to starch prior to extrusion. As a matter of fact, control samples extruded at 100, 120 or 140 °C barrel temperatures exhibited a mixture of A and V patterns whereas at 160 °C exhibited the V-pattern. On the other hand starch–myristate extrudates extruded at 100 or 120 °C and starch–palmitate extrudates extruded at 100 °C barrel temperature exhibited A and V mixed patterns whereas starch–fatty acid extrudates extruded at barrel temperatures higher than the previously mentioned exhibited the V-pattern.

Fig. 6 shows the percentage relative crystallinity exhibited by both control and starch–fatty acid extrudate samples as a function of barrel temperature and screw speed. It can be seen that the crystallinity of the control samples substantially diminished as both the screw speed and the barrel temperature increased. Similarly, the crystallinity of starch–fatty acid extrudates diminished with the increase of barrel temperature and screw speed, however their crystallinity was always much higher than that of the control samples. This reduction in crystallinity could be explained as follows: it is well established (Biliaderis & Seneviratne, 1990; Raphaelides & Karkalas, 1988; Stute & Konieczny-Janda, 1983) that amylose, at temperatures close to 100 °C, forms with lipids crystalline complexes whose dissociation temperature is around 120 °C, depending on the availability of water present. If the complexes are heat treated over their dissociation temperature and then cooled very rapidly, they will be reformed to a lesser degree. In the present work it can be seen (Fig. 6) that at low barrel temperatures, i.e. below the dissociation temperature of the complexes and at fairly low screw speeds, i.e. allowing sufficient time the amylose–lipid interaction to take place and to form as much compact as possible crystallites, the crystallinity of extrudates is fairly high. However, as the barrel temperature increases which means the complexes tend to dissociate and the screw speed increases, the complexes

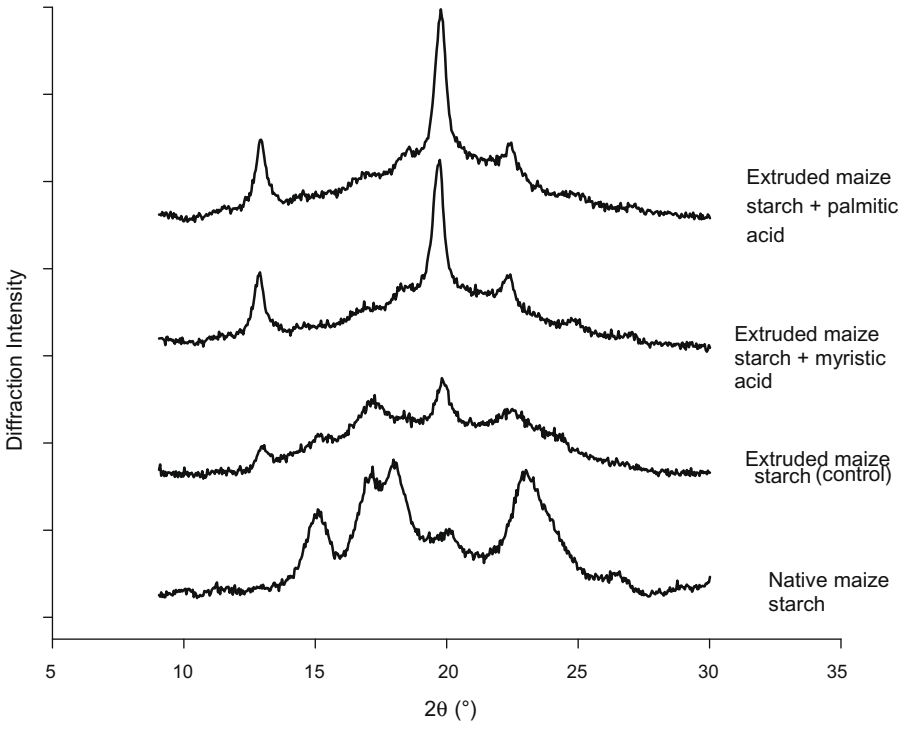

Fig. 5. X-ray diffraction patterns of maize starch either native or extruded with the addition of fatty acid or with out at 140 °C barrel temperature and at 227 rpm screw speed.

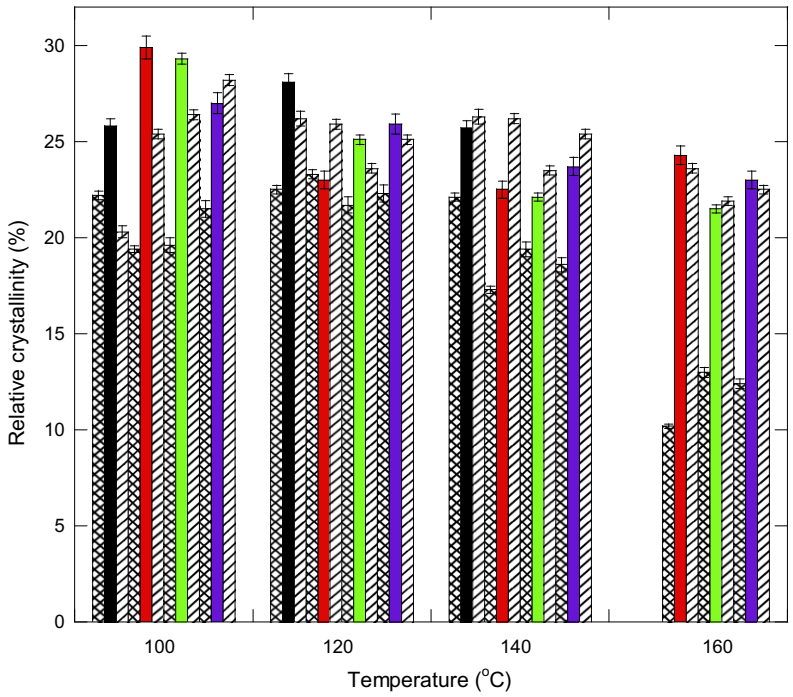

Fig. 6. Effect of screw speed and barrel temperature on the relative crystallinity of starch–fatty acid extrudates. Symbols are the same as in Fig. 2.

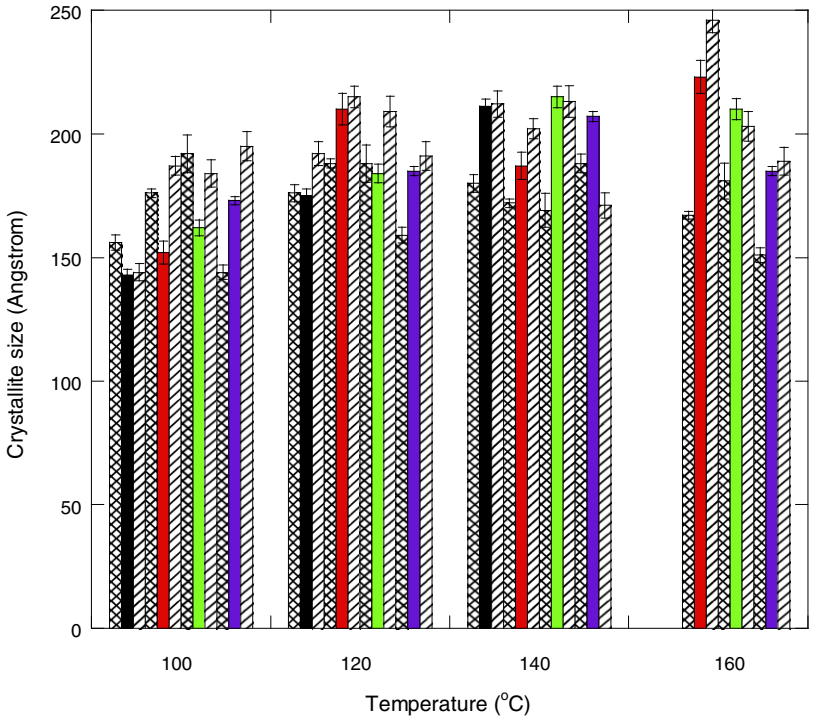

Fig. 7. Effect of screw speed and barrel temperature on the crystallite size of starch–fatty acid extrudates. Symbols are the same as in Fig. 2.

were only partly reformed due to very short times of being under ideal conditions for their reformation. As for the crystallite size of the extrudate samples, Fig. 7 shows that it is rather barrel temperature dependent than screw speed dependent. It can be seen that crystallite size attained the maximum value in rather higher barrel temperatures. This could be attributed to a kind of annealing process which might take place helping in the formation of more compact crystalline complexes (possibly IIb polymorph structure), hence with bigger crystallite size. Again, in most cases the size of crystallites of the starch–fatty acid extrudates was bigger than that of the crystallites of the control samples. Since the A-type crystalline structure of native starch gradually has been destroyed during extrusion, the residual crystallinity of the control samples should be mainly due to that of the amylose–native lipid interaction

whose quantity was very small comparing to the amount of fatty acid intentionally added to starch. Thus, both crystallinity and crystallite size of the control samples were lower than those of the starch–fatty acid extrudates, where the quantity of fatty acid added to starch was more than sufficient to interact with all the available amylose molecules. Moreover, it is noteworthy to point out how fast was the amylose–fatty acid interaction if we consider that the whole extrusion process especially at high screw speed, i.e. 227 rpm did not last more than 25–30 s (estimated using the dye technique).

3.7. Thermomechanical analysis

Dynamic mechanical testing of starch extrudates under programmed heating is considered as an appropriate method to determine the glass transition temperature (T_g) of these products. All extrudate samples examined in this work were very rigid as well as brittle thus they were very difficult to handle during oscillation experiments. Fig. 8 shows the changes in the modulus of elasticity (G') of starch extrudates in relation to barrel temperature and screw speed. It can be seen (Fig. 8a) that at 20 rpm screw speed the control samples were more rigid than the starch–fatty acid extrudates. Similar behaviour was observed at 91 rpm screw speed for barrel temperatures 100 and 120 °C whereas for barrel temperatures 140 and 160 °C the rigidity of starch–fatty acid extrudates became higher than that of the control. At 161 rpm screw speed the rigidity of the control at 100 °C barrel temperature was much less than those of the starch–fatty acid extrudate samples (Fig. 8b). On the other hand at barrel temperatures 120, 140 and 160 °C the rigidity of control samples was higher than those of the starch–fatty acid extrudates. As for the samples obtained at screw speed 227 rpm and barrel temperatures 100 and 120 °C the rigidity was the same for all samples examined whereas at barrel temperatures 140 and 160 °C the rigidity of starch–fatty acid extrudates was similar or lower than that of the control (Fig. 8c). The mechanical behaviour exhibited by the samples examined was puzzling and difficult to explain.

Glass transition temperature was determined from the position of tan δ peak observed for most of the extrudates. It can be seen (Table 3) that with the exception of control samples extruded at 100 °C barrel temperature whose T_g values ranged from 66 up to 76 °C, most of the other samples exhibited T_g values ranged from 80 to 90 °C, which explains why they were very brittle and relatively easy to fracture. Since it has been reported (Brent, Mulvaney, Cohen, & Bartsch, 1997) that water is a very effective plasticizer whose presence reduces the T_g of extrudates, a comparison of

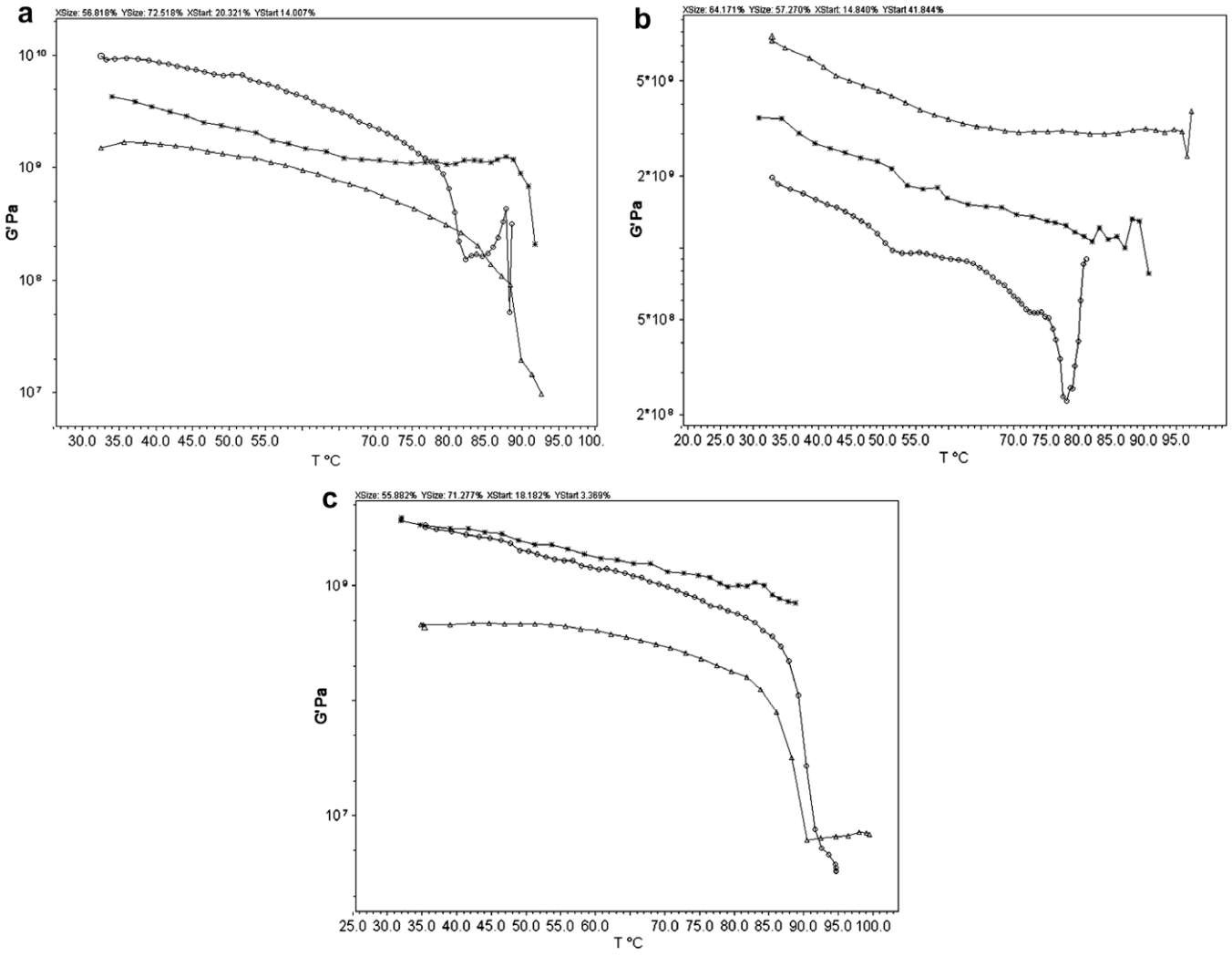

Fig. 8. Storage modulus (G') versus temperature of heating of starch extruded with the addition of fatty acids or without (control), at various barrel temperatures and screw speeds. (a) Samples extruded at 100 °C and at 20 rpm screw speed; (b) samples extruded at 100 °C and at 161 rpm; (c) samples extruded at 140 °C and at 227 rpm; symbols: O, control, ∗, myristic acid, Δ palmitic acid. Frequency of oscillation, 0.1 Hz; stress applied, 150 Pa; heating rate, 5 °C/min.

Table 3
Glass transition temperature (T_g) of maize starch–fatty acid extrudates.

Sample	Barrel temperature (°C)	Screw speed (rpm)	T_g (°C)
Control	100	20	76 ± 2.0
''	''	91	73 ± 1.0
''	''	161	66 ± 3.0
''	''	227	69 ± 3.0
Starch + myristate	''	20	89 ± 4.0
''	''	91	82 ± 1.0
''	''	161	73 ± 2.0
''	''	227	80 ± 3.0
Starch + palmitate	''	20	75 ± 0.5
''	''	91	81 ± 1.0
''	''	161	Not observed
''	''	227	85 ± 2.0
Control	120	20	80 ± 0.5
''	''	91	74 ± 2.0
''	''	161	80 ± 1.0
''	''	227	84 ± 3.0
Starch + myristate	''	20	90 ± 2.0
''	''	91	89 ± 1.0
''	''	161	81 ± 2.0
''	''	227	68 ± 5.0
Starch + palmitate	''	20	90 ± 4.0
''	''	91	86 ± 2.0
''	''	161	64 ± 6.0
''	''	227	Not observed
Control	140	20	85 ± 2.0
''	''	91	85 ± 4.0
''	''	161	90 ± 2.0
''	''	227	Not observed
Starch + myristate	''	20	90 ± 2.0
''	''	91	90 ± 1.0
''	''	161	81 ± 4.0
''	''	227	68 ± 3.0
Starch + palmitate	''	20	88 ± 2.0
''	''	91	82 ± 4.0
''	''	161	Not observed
''	''	227	75 ± 2.0
Control	160	91	Not observed
''	''	161	Not observed
''	''	227	90 ± 1.0
Starch + myristate	''	91	92 ± 3.0
''	''	161	58 ± 2.0
''	''	227	89 ± 3.0

moisture content data for the control samples (Table 2) and the corresponding T_g data from Table 3 more or less verifies the above statement. However, the moisture content of the other samples was not relatively low thus it should have been expected these samples to have lower T_g values, than actually they had. That means, the water molecules mobility has been effectively constrained in the structural matrix of the extrudates and they were not available to facilitate the motion of the macromolecular chains which were present in their domain. To act as plasticizer water molecules should be present mainly in the amorphous regions of the starch system matrix. In the case of the extrudate samples of the present work, the high T_g values observed, possibly means that part of the water present should have been effectively trapped within the interstices of the crystallites formed during the extrusion process thus rendering these water molecules practically unavailable to participate in the plasticization of the starch system.

4. Conclusions

The results of this work indicated that starch–fatty acid interactions which take place during extrusion cooking of starch in the presence of added fatty acids do affect the characteristics of starch extrudates even in the melt state. That is, during extrusion, the presence of lipids caused reduction to SME input provided by the extruder motor thus helping in reducing both mechanical wear of the extruder as well as in saving energy. On the other hand the crystallinity of the formed extrudates was increased due to the presence of fatty acids with the result their structure to become very rigid. The most pronounced effects of these interactions are the reduction in water solubility and the textural modification. These effects are related to processing conditions employed.

Acknowledgments

We are thankful to Evaggelos Tellos and Christos Bounarelis for their technical assistance during the running of the extruder and to Dr. Ioannis Arvanitidis for helpful discussions concerning the treatment of the crystallographic data.

The financial support received from the European Union-Greek Ministry of Education through the "ARCHIMEDES" research program is gratefully acknowledged.

References

Anderson, R. A., Conway, H. F., Pfeifer, V. F., & Griffin, L. E. J. (1969). Gelatinization of corn grits by roll- and extrusion cooking. *Cereal Science Today, 14*(4–7), 11–12.
Banks, W., & Greenwood, C. T. (1971). The conformation of amylose in dilute solution. *Stärke, 23*, 300–314.
Bhatnagar, S., & Hanna, M. A. (1994). Extrusion processing conditions for amylose–lipid complexing. *Cereal Chemistry, 71*, 587–593.
Bhatnagar, S., & Hanna, M. A. (1997). Modification of microstructure of starch extruded with selected lipids. *Starch/Stärke, 49*, 12–20.
Biliaderis, C. G., & Seneviratne, H. D. (1990). On the supermolecular structure and metastability of glycerol monostearate–amylose complex. *Carbohydrate Polymers, 13*, 185–206.
Birch, G. G., & Priestly, R. J. (1973). Degree of gelatinization of cooked rice. *Stärke, 25*, 98–100.
Bizot, H. (1983). Using the "G.A.B." model to construct sorption isotherms. In R. Jowitt, F. Escher, B. Hallström, H. F. T. Meffert, W. E. L. Spiess, & G. Vos (Eds.), *Physical properties of foods* (pp. 43–54). London: Applied Science Publishers.
Brent, J. L., Mulvaney, S. J., Cohen, S., & Bartsch, J. A. (1997). Thermomechanical glass transition of extruded cereal melts. *Journal of Cereal Science, 26*, 301–312.
Brundle, R. C., Evans, C. A., & Wilson, S. (1992). *Encyclopedia of materials characterization – Surfaces interfaces, thin films*. Boston: Butterworth–Heinemann.
Cai, W., & Diosady, L. L. (1993). Model for gelatinization of wheat starch in a twin-screw extruder. *Journal of Food Science, 58*, 872–887.
Carlson, T. L.-G., Larsson, K., Dinh-Nguyen, N., & Krog, N. (1979). A study of the amylose–monoglyceride complex by Raman spectroscopy. *Stärke, 31*, 222–224.
Colonna, P., Doublier, J. L., Melcion, J. P., de Monredon, F., & Mercier, C. (1984). Extrusion cooking and drum drying of wheat starch. I. Physical and macromolecular modifications. *Cereal Chemistry, 61*, 538–543.
Colonna, P., & Mercier, C. (1983). Macromolecular modifications of manioc components by extrusion-cooking with and without lipids. *Carbohydrate Polymers, 3*, 87–108.
Davidson, V. J., Paton, D., Diosady, L. L., & Larocque, G. (1984). Degradation of wheat starch in a single screw extruder: Characteristics of extruded starch polymers. *Journal of Food Science, 49*, 453–458.
Della Valle, G., Kozlowski, A., Colonna, P., & Tayeb, J. (1989). Starch transformation estimated by the energy balance on a twin-screw extruder. *Lebensmittel Wissenschaft und Technologie, 22*, 279–286.
Godet, M. C., Tran, V., Delage, M. M., & Buleon, A. (1993). Molecular modelling of the specific interactions involved in the amylose complexation by fatty acids. *International Journal of Biological Macromolecules, 15*, 11–16.
Greenwood, C. T. (1964). Viscosity–molecular weight relations. In: R. L. Whistler (Ed.), *Methods in carbohydrate chemistry: Vol. IV. Starch* (pp. 179–188). USA: Academic Press.
Han, C. D. (1976). *Rheology in polymer processing*. USA: Academic Press (pp. 89–126).
Karkalas, J. (1985). An improved enzymic method for the determination of native and modified starch. *Journal of the Science of Food and Agriculture, 36*, 1019–1027.

Karkalas, J., & Raphaelides, S. (1986). Quantitative aspects of amylose–lipid interactions. *Carbohydrate Research, 157*, 215–234.

Launay, B., & Konê, T. (1984). Twin-screw extrusion cooking of corn starch: Flow properties of starch pastes. In P. Zeuthen, J. C. Cheftel, C. Eriksson, M. Jul, H. Leniger, & P. Linko, et al. (Eds.), *Thermal processing and quality of foods* (pp. 54–61). England: Elsevier Applied Science Publishers.

Mercier, C. (1980). Veraenderungen der Struktur und Verdaulichkeit von Getreidestärken beim Extrudieren. *Getreide Mehl und Brot, 34*, 52–58.

Mercier, C., Charbonniere, R., Grebaut, J., & de la Gueriviere, J. F. (1980). Formation of amylose–lipid complexes by twin-screw extrusion cooking of manioc starch. *Cereal Chemistry, 57*, 4–9.

Meuser, F., van Lengerich, B., & Stender, J. (1985a). Bildung von Stärkelipidkomlpexen durch Kochextrusion. 1 Teil: Herstellung und strukturelle Charakterisierung der Komplexe. *Getreide Mehl und Brot, 39*, 205–211.

Meuser, F., van Lengerich, B., & Stender, J. (1985b). Bildung von Stärkelipidkomlpexen durch Kochextrusion. 2 Teil: Funktionelle Eigenschaften der Extrudate. *Getreide Mehl und Brot, 39*, 309–314.

Morrison, W. R., & Laignelet, B. (1983). An improved colorimetric procedure for determining apparent and total amylose in cereal and other starches. *Journal of Cereal Science, 1*, 9–20.

Parker, R., Ollett, A.-L., & Smith, A. C. (1990). Starch melt rheology: Measurement, modeling and applications to extrusion processing. In P. Zeuthen (Ed.). *Processing and quality of foods* (Vol. 1, pp. 1290–1295). England: Elsevier Applied Science Publishers.

Raphaelides, S., & Karkalas, J. (1988). Thermal dissociation of amylose–fatty acid complexes. *Carbohydrate Research, 172*, 65–82.

Raphaelides, S. N. (1992). Flow behaviour of starch–fatty acid systems in solution. *Lebensmittel Wissenschaft und Technologie, 25*, 95–101.

Raphaelides, S. N., & Georgiadis, N. (2006). Effect of fatty acids on the rheological behaviour of maize starch dispersions during heating. *Carbohydrate Polymers, 65*, 81–92.

Snape, C. E., Morrison, W. R., Maroto-Valer, M. M., Karkalas, J., & Pethrick, R. A. (1998). Solid state ^{13}C NMR investigation of lipid ligands in V-amylose inclusion complexes. *Carbohydrate Polymer, 36*, 225–237.

Stäger, G. (1988). *Über die Interaktionen von Emulgatoren mit Stärke bei der Heissextrusion*. Doctoral dissertation. Zürich: Eidgenössischen Technischen Hochschule Zürich.

Stribeck, N. (2007). *X-ray scattering of soft matter*. Berlin: Springer.

Stute, V. R., & Konieczny-Janda, G. (1983). DSC-untersuchungen an stärken. II. Untersuchungen an stärke–lipid komplexen. *Stärke, 35*, 340–347.

van Lengerich, B. (1989). Influence of extrusion processing on in-line rheological behavior, structure and function of wheat starch. In H. Faridi & J. M. Faubion (Eds.), *Dough rheology and baked product texture* (pp. 421–471). New York: Avi Publishing.

Willett, L. J., Jasberg, K. B., & Swanson, L. C. (1995). Rheology of thermoplastic starch: Effects of temperature, moisture content and additives on melt viscosity. *Polymer Engineering and Science, 35*(2), 202–210.